

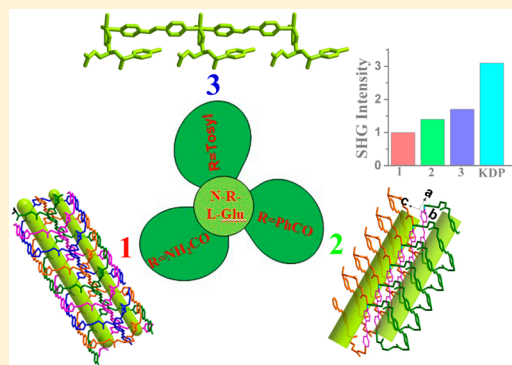
From Pair Quadruple- to Single-Stranded Helices to Lines in a Mixed Ligand System via Adjusting the N-Substituent of L-Glu

Yuehong Wen, Tianlu Sheng, Zhenzhen Xue, Yong Wang, Chao Zhuo, Xiaoquan Zhu, Shengmin Hu, and Xintao Wu*

State Key Laboratory of Structure Chemistry, Fujian Institute of Research on the Structure of Matter, Chinese Academy of Sciences, Fuzhou, 350002, China

Supporting Information

ABSTRACT: Utilizing the mixed-ligand strategy, a novel fourfold-interpenetrated 3D homochiral metal–organic framework (1) with rare pair quadruple-stranded helices was assembled from bpee (1,2-bis(4-pyridyl)ethylene) and NCG (N-carbamyl-L-glutamate). Changing the carbamyl substituent of NCG with benzoyl group (NBzG: N-benzoyl-L-glutamate), a non-interpenetrated 3D homochiral coordination polymer (2) composed of alternate right-handed and left-handed single helix was obtained. When *p*-tolylsulfonyl substituent was used instead, an interesting homochiral linear structure (3) was formed from mixed-ligand bpee and NTsG (N-*p*-tolylsulfonyl-L-glutamate), with all individual NTsG being lined up orderly. The steric hindrance of N-substituent of L-glu has a tremendous impact on the construction of these diverse frameworks. Complexes 1–3 display second harmonic generation (SHG) efficiencies, which are approximately 0.32, 0.45, and 0.55 times as much as that of KDP powder.



INTRODUCTION

Chirality and helicity are essential to biological functions,^{1,2} playing a very important role in the living processes. In recent years, the homochiral and helical coordination polymers (CPs) or metal–organic frameworks (MOFs) have attracted increasing attention not only because of their intriguing architectures, but also because of their potential applications such as asymmetric catalysis,³ enantioselective sorption and separations,⁴ and so forth.⁵ Up to now, many strategies and methodologies have been developed to design and prepare homochiral CPs, including the usage of chiral building blocks or chiral auxiliary,⁶ asymmetric crystallization from achiral precursors (chiral induction),⁷ and so forth.⁸ Helicity often goes with chirality, so various fascinating helical chains have also been found in such homochiral CPs. Nonetheless, it is a great challenge to design and construct helical structures predictably because of the uncontrollability of the assembly process. The mixed-ligand approach should be considered as an attractive strategy to prepare helical structures. For example, carboxylate combined with an N-donor ligand has been proven successful in construction of numerous helical CPs.⁹ Usually, V-shaped ligands (dicarboxylate or bis(pyridine)) have been employed.¹⁰ The cooperation of chiral linear dicarboxylates and linear rigid N-donor ligands to prepare homochiral CPs with helical motifs has been less explored.¹¹ Most recently, a series of homochiral two-dimensional (2D) coordination polymers with different helical chains have been self-assembled from a chiral linear dicarboxylate and three achiral flexible bis(pyridine)

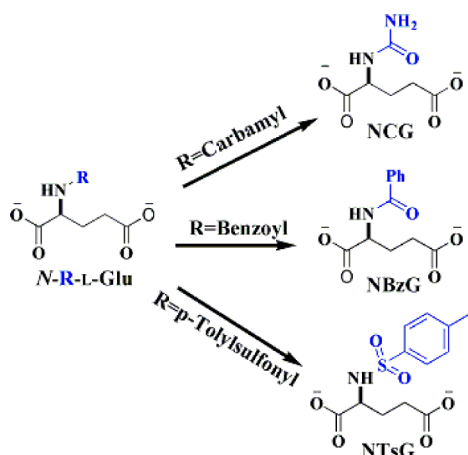
ligands.¹² In order to further develop the related research, we focus on the synthesis of homochiral CPs with more diverse frameworks (3D and 1D) and helix, from mixed ligand of a linear rigid bis(pyridine) ligand and varied chiral linear dicarboxylates.

Trans-1,2-bis(4-pyridyl)ethylene, a rigid linear N-donor ligand, is powerful in the field of coordination chemistry. By cooperating with different dicarboxylates, a great number of CPs has been assembled. Among these examples, using the mixed ligand of a chiral dicarboxylate and bpee to prepare homochiral CPs has been poorly studied.¹³ On the other hand, L-glutamic acid (L-glu) is a cheap chiral material, having two carboxylic acid groups and one amine. Transformation the free amino group to amide can make the coordination mode simpler and avoid the side reaction between the amine and remote acid of L-glu. When N-R-L-glu reacts with metals, it can function as a simple chiral dicarboxylate linker.^{14,12} By combining bpee with N-R-L-glu, to self-assemble with Zn(II) ions, some novel homochiral frameworks with diverse helical chains should be obtained. More importantly, the frameworks and helix may be altered through adjusting the geometric size of the N-substituent group of L-glu. We report herein the syntheses, structural characterization, chirality, and nonlinear optical properties of three homochiral coordination polymers from bpee and three L-glu derivatives (Scheme 1).

Received: January 20, 2015

Published: April 8, 2015

Scheme 1. Structures of the Derivatives of L-Glutamate



EXPERIMENTAL SECTION

Materials and Methods. L-Glu derivatives (NCGA: N-carbamyl-L-glutamic acid; NBzGA: N-benzoyl-L-glutamic acid; NTsGA: N-p-tolylsulfonyl-L-glutamic acid), bpee, $\text{Zn}(\text{NO}_3)_2 \cdot 6\text{H}_2\text{O}$, and solvents were purchased commercially and used directly. All manipulations were carried out under aerobic and mild conditions. Elemental analyses (C, H, and N) were performed with a Vario MICRO CHNOS Elemental Analyzer. The infrared spectra with KBr pellets were recorded in the range of 4000–400 cm^{-1} on a PerkinElmer Spectrum One FT-IR Spectrometer. Powder X-ray diffraction (PXRD) data were collected on a DMAX-2500 diffractometer with $\text{Cu K}\alpha$. Circular dichroism (CD) spectra were conducted on a Jasco J-810 spectrodichromometer. SHG measurements on powder samples of CPs 1–3 and KDP were carried out by the Kurtz and Perry method using a Nd:YAG laser (1064 nm).

Synthesis of $[\text{Zn}(\text{bpee})(\text{NCG}) \cdot 1.5\text{H}_2\text{O}]_n$ (1). A solution of bpee (55 mg, 0.3 mmol) and $\text{Zn}(\text{NO}_3)_2 \cdot 6\text{H}_2\text{O}$ (90 mg, 0.3 mmol) in $\text{H}_2\text{O}/\text{EtOH}/\text{DMF}$ (6 mL/3 mL/2 mL) was stirred for 10 min. Then, a solution of NCGA (57 mg, 0.3 mmol) and 1 N NaOH (0.6 mL) in $\text{H}_2\text{O}/\text{EtOH}$ (2 mL/4 mL) was added carefully over it. Colorless long needlelike crystals were collected after one month. Yield: 122 mg, 88%.

Elemental analysis calcd (%) for $\text{C}_{18}\text{H}_{21}\text{N}_4\text{O}_{6.5}\text{Zn}$: C 46.72, H 4.57, N 12.11; found: C 45.90, H 5.10, N 11.81. IR (solid KBr pellet, ν/cm^{-1}) 3477 (w), 3358 (m), 2944 (w), 2468 (vw), 1645 (w), 1619 (s), 1526 (m), 1438 (m), 1412 (s), 1396 (s), 1298 (s), 1260 (m), 1142 (w), 1066 (m), 1024 (m), 978 (w), 835 (s), 790 (w), 750 (w), 622 (m), 549 (s).

Synthesis of $[\text{Zn}(\text{bpee})(\text{NBzG})]_n$ (2). Prepared as described for 1 except that NBzGA was used instead of NCGA. Colorless needlelike crystals were collected after three months. Yield: 120 mg, 81%. Elemental analysis calcd (%) for $\text{C}_{24}\text{H}_{21}\text{N}_3\text{O}_5\text{Zn}$: C 58.02, H 4.26, N 8.46; found: C 57.63, H 4.38, N 8.38. IR (solid KBr pellet, ν/cm^{-1}) 3350 (s), 3058 (w), 3033 (w), 2915 (w), 2459 (vw), 1636 (s), 1611 (s), 1522 (m), 1484 (m), 1421 (s), 1362 (s), 1341 (s), 1303 (s), 1282 (s), 1252 (w), 1214 (m), 1201 (w), 1100 (m), 1062 (m), 1024 (s), 957 (m), 830 (s), 775 (w), 729 (m), 695 (m), 636 (w), 568 (m), 551 (s), 463 (m).

Synthesis of $[\text{Zn}(\text{bpee})(\text{NTsG})(\text{H}_2\text{O})_2]_n$ (3). Prepared as described for 1 except that NTsGA was used instead of NCGA. Colorless bulk crystals were collected after three months. Yield: 145 mg, 83%. Elemental analysis calcd (%) for $\text{C}_{24}\text{H}_{27}\text{N}_3\text{O}_8\text{SZn}$: C 49.45, H 4.67, N 7.21; found: C 49.37, H 4.77, N 7.19. IR (solid KBr pellet, ν/cm^{-1}) 3358 (m), 3282 (m), 2890 (w), 2307 (vw), 1602 (s), 1556 (s), 1539 (s), 1459 (m), 1421 (s), 1391 (s), 1320 (s), 1290 (m), 1305 (w), 1197 (w), 1155 (s), 1092 (s), 1011 (m), 973 (s), 919 (m), 826 (s), 809 (s), 775 (w), 703 (m), 653 (s), 547 (s), 509 (w), 484 (m).

Single-Crystal Structure Determination. The X-ray single crystal structure analyses for compounds 1–3 were performed on a Rigaku SCXmini diffractometer (Mo $\text{K}\alpha$ radiation, $\lambda = 0.71073 \text{ \AA}$, graphite monochromator) at 293(2) K. Empirical absorption corrections were applied to the data using the SADABS program.¹⁵ The structures were solved by the direct method and refined by the full-matrix least-squares on F^2 using the SHELXL-97 program.¹⁶ All of the non-hydrogen atoms were refined anisotropically, and the hydrogen atoms attached to carbon were located at their ideal positions. Crystal data for 1–3 are presented in Table 1. Selected bond lengths and angles of 1–3 are listed in Tables S1–S3 of the Supporting Information.

RESULTS AND DISCUSSION

Description of Crystal Structures. *Crystal Structure of $[\text{Zn}(\text{bpee})(\text{NCG}) \cdot 1.5\text{H}_2\text{O}]_n$ (1).* Complex 1 crystallizes in the

Table 1. Crystal Data and Refinement Results for Complexes 1–3

compound	1	2	3
Empirical formula	$\text{C}_{72}\text{H}_{84}\text{N}_{16}\text{O}_{26}\text{Zn}_4$	$\text{C}_{96}\text{H}_{84}\text{N}_{12}\text{O}_{20}\text{Zn}_4$	$\text{C}_{24}\text{H}_{27}\text{N}_3\text{O}_8\text{SZn}$
<i>M</i>	462.76	496.81	582.92
Crystal system	orthorhombic	monoclinic	triclinic
Space group	$P2_12_12$	$P2_1$	$P1$
Flack parameter	0.03(1)	0.07(1)	0.02(1)
<i>a</i> (Å)	17.655(7)	5.2954(6)	5.737(4)
<i>b</i> (Å)	21.733(8)	21.7207(18)	9.220(6)
<i>c</i> (Å)	5.626(2)	18.731(2)	11.957(8)
α (deg)	90	90	79.343(16)
β (deg)	90	97.633(8)	85.956(13)
γ (deg)	90	90	88.690(19)
$V/\text{\AA}^3$	2158.6(13)	2135.3(4)	619.9(7)
<i>Z</i>	4	4	1
<i>D</i> /g cm^{-3}	1.424	1.545	1.561
μ/mm^{-1}	1.180	1.193	1.130
θ_{range} (deg)	2.3072–27.5283	2.1716–27.4547	2.2479–27.5205
<i>h, k, l</i> , ranges	–22 to 22, –28 to 27, –7 to 7	–6 to 6, –28 to 28, –14 to 23	–7 to 7, –11 to 11, –15 to 15
<i>F</i> (000)	956	1024	302
$R_1,^a wR_2,^b [I > 2\sigma(I)]$	0.0446, 0.1427	0.0711, 0.1149	0.0323, 0.0524
GOF on F^2	1.084	0.967	0.896

$$^a R = \sum (||F_o| - |F_c||) / \sum |F_o|. \quad ^b wR = \{ \sum w[(F_o^2 - F_c^2)^2] / \sum w[(F_o^2)^2] \}^{1/2}.$$

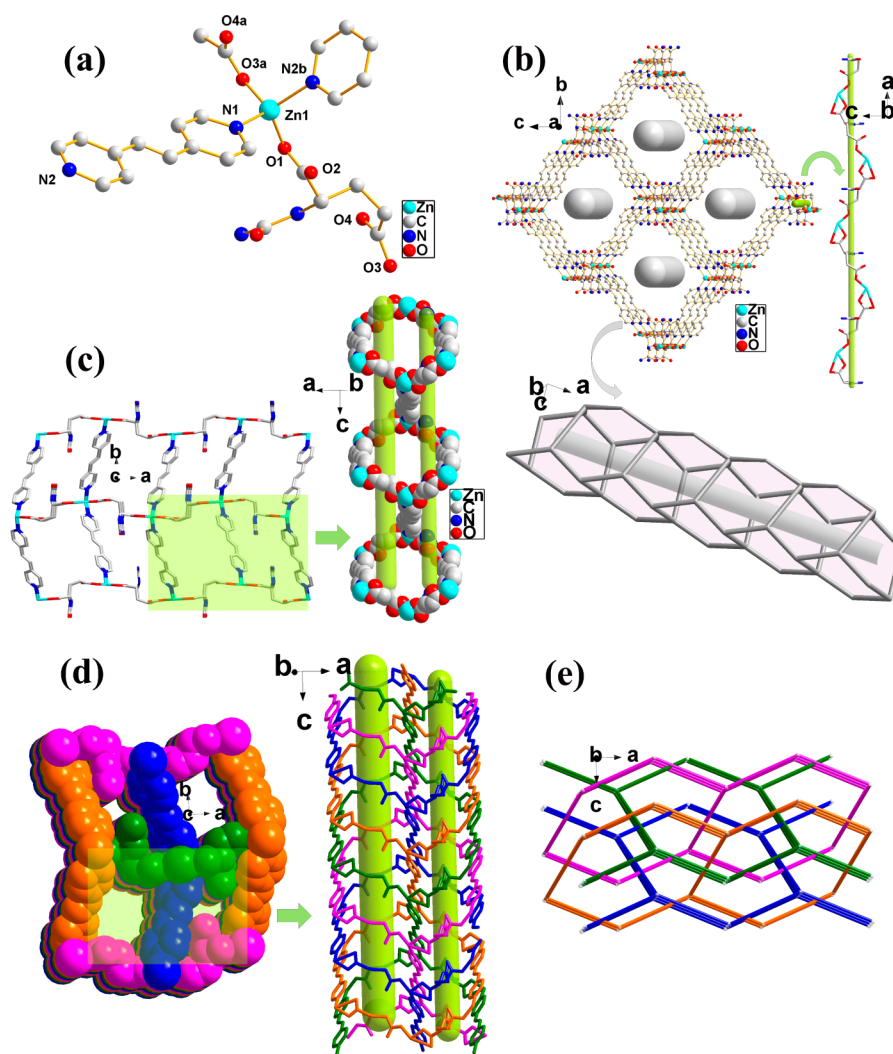


Figure 1. (a) Coordination configurations of Zn(II) atom (hydrogen atoms and disordered oxygen atoms have been omitted for clarity). Symmetry code: (a) $x - 1/2, -y + 1/2, -z + 1$; (b) $-x + 3/2, y - 1/2, -z - 1$. (b) Single 3D structure of **1** viewed down the *a* axis, left-handed helical chain composed of NCG (right), and 1D nanotubular channels (below). (c) Single 3D structure of **1** viewed down the *c* axis and a pair of helical chains. (d) Fourfold-interpenetrated 3D framework of **1** with pair quadruple-stranded helices. (e) Topological net.

orthorhombic space group $P2_12_12$ with flack parameters of 0.03 (1); its asymmetric unit consists of one Zn(II), one bpee, one NCG, and one and a half uncoordinated water molecules (Figure 1a). All the Zn(II) ions are four-coordinated by two O atoms (O1 and O3a) of carboxylate groups from two separate NCG and two N atoms (N1 and N2b) of two different bpee ligands, forming a distorted tetrahedral coordination geometry. The bond lengths of Zn–N are 2.030(3) and 2.037(3) Å, and the two Zn–O distances are 1.936(3) and 1.964(3) Å, respectively. The Zn···Zn distance spanned by one NCG and one bpee is 9.85(1) and 13.41(1) Å, respectively. The bond angles around Zn(II) ions vary from 98.9(1)° to 114.1(1)°. The NCG ligands are linked by Zn(II) ions to form a 1D left-handed helical chain with the pitch of 17.66 Å along the *a* axis (Figure 1b). The bpee connected those helical chains via Zn–N coordination bonds to form a 3D framework with 1D nanotubular channels along the *a* axis (Figure 1b). A pair of similar helical chains was observed viewed down the *c* axis: one is left-handed with the carbamido groups directed outward from the spiral channel; the other is right-handed with all carbamido groups pointed inward. Both helical pitches are 22.49 Å (Figure 1c). Such a single 3D structure with large

windows is unstable except by interpenetration or by incorporation of appropriate guests. So, a homochiral fourfold-interpenetrated 3D metal–organic framework compound is given, in order to minimize the large void cavities and stabilize the framework. Meanwhile, a pair of quadruple-helices is also formed (Figure 1d). To the best of our knowledge, there have been few reports on such a pair of quadruple helices.¹⁷ Various hydrogen bonds exist between neighboring helical chains (Figure S1, Supporting Information), with bond lengths varied from 2.39 to 2.81 Å. Topologically, the 3D network can be described as a four-connected fourfold interpenetrating diamond net with a point symbol $\{6^6\}$ (Figure 1e).

Crystal Structure of $[Zn(bpee)(NBzG)]_n$ (2**).** Complex **2** crystallizes in the chiral monoclinic space group $P2_1$, with flack parameters of 0.07(1). The asymmetric unit consists of one Zn(II), one bpee, and one NBzG (Figure 2a). Both Zn1 and Zn2 adopt a distorted tetrahedral coordination geometry, which is completed by two O (O1, O6 and O3, O8a, respectively) atoms from two NBzG ligands and two N (N1, N4 and N2b, N5c, respectively) atoms from two bpee ligands. The bond lengths of Zn–O and Zn–N are 1.897(5) to 2.061(7) Å. The bond angles around Zn(II) ions vary from 93.4(2)° to

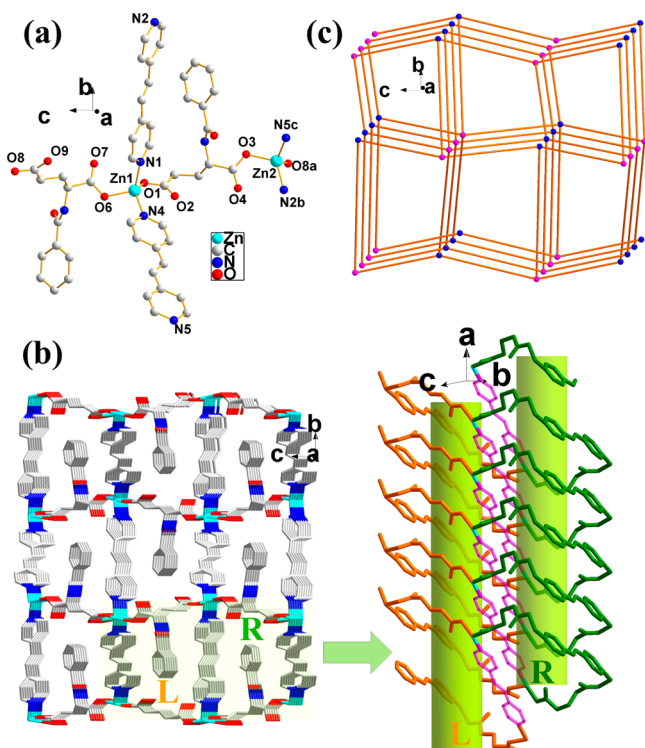


Figure 2. (a) Coordination configurations of Zn(II) atom (hydrogen atoms have been omitted for clarity). Symmetry code: (a) $x - 1, y, z - 1$; (b) $-x, y - 1/2, -z - 2$; (c) $-x + 1, y + 1/2, -z - 2$. (b) 3D structure of **2** viewed down the a axis, with left-handed and right-handed helical chains arranged alternately. (c) Topological net.

$129.1(3)^\circ$. The Zn \cdots Zn distances spanned by one bpee ligand and one NBzG ligand are 13.44(1) and 13.48(1) Å, 9.30(1) and 10.12(1) Å, respectively. Complex **2** shows a homochiral 3D structure possessing two kinds of helical chains, in which the left-handed and right-handed helical chains are in an alternate arrangement along the c axis by sharing the bpee ligands (Figure 2b). The helical pitches are 5.29 Å, according to the length of the a axis. All the helical channels are occupied by the phenyl groups of NBzG. There exist many hydrogen bonds

(aromatic H \cdots O and N—H \cdots O), with bond lengths varied from 2.23 to 2.83 Å (Figure S2, Supporting Information). Considering each metal a node, the 3D network of **2** can be described as a four-connected CdSO $_4$ -like framework with a point symbol $\{6^5.8\}$ (Figure 2c).

Crystal Structure of [Zn(bpee)(NTsG)(H $_2$ O) $_2$] $_n$ (3**).** The single-crystal X-ray diffraction study revealed that complex **3** crystallizes in the chiral triclinic space group $P1$ with flack parameters of 0.02(1). Its asymmetric units contain one Zn(II), one bpee, one NTsG, and two coordinated water molecules (Figure 3a). The Zn(II) center adopts a distorted octahedral coordination configuration completed by four O atoms from one carboxylate of NTsG (O1 and O2) and two water molecules (O7 and O8) composing the equatorial plane, and two N (N1 and N2a) atoms from bpee at the apical position. The other carboxylate of NTsG is uncoordinated. The selected bond length and angles are listed in Table S3. The Zn \cdots Zn distances spanned by one bpee are 13.68(1) Å. The bpee ligand functions as a bridging linker, connecting different Zn(II) to form an infinite linear chain. The chiral NTsG ligands dock at each Zn(II) center orderly, which causes complex **3** to have homochirality (Figure 3b). Different lines of **3** are piled into a 2D layer through varied intermolecular hydrogen bonding interactions (Figure 3c). The lengths of hydrogen bonds vary from 2.39 to 2.76 Å. Adjacent layers are stacked in an AA type arrangement. There have three intermolecular hydrogen bonds (aromatic-H \cdots O) and the lengths of hydrogen bonds are 2.49, 2.57, and 2.61 Å. As a result, a 3D architecture of complex **3** was formed (Figure 3d).

Comparison of the Structures. The achiral ligand bpee displays similar linear conformations and functions as a bridging linker, connecting different Zn(II) to form zigzag chains in complexes **1** and **2**, and a linear chain in complex **3**. The chiral dicarboxylate ligands NCG, NBzG, and NTsG adopt different conformations and coordination modes. In complex **1**, the NCG acts as a simple bidentate bridge, to link Zn(II) ions via two monodentate carboxyl groups to form a 1D left-handed helical chain. Similarly, the NBzG in complex **2** acts as a simple bidentate bridge as well; however, the $-(CH_2)_3-$ chains show two different types of configurations (*anti-anti* vs *syn-anti*,

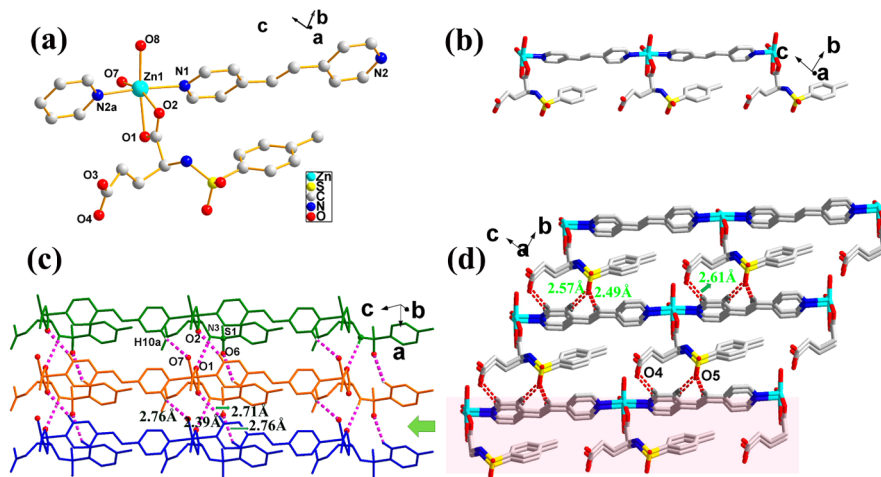
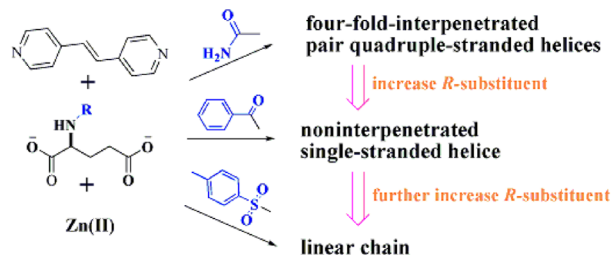


Figure 3. (a) Coordination configurations of Zn(II) atom (hydrogen atoms have been omitted for clarity). Symmetry code: (a) $x, y - 1, z + 1$. (b) Linear chain of **3**. (c) 2D layer of **3** composed of different chains through intermolecular hydrogen bonding interactions (purple dashed lines represent the intermolecular hydrogen bonds). (d) 3D structure of **3** viewed down the a axis (red dashed lines represent the intermolecular hydrogen bonds).

Figure S3, Supporting Information), whereas in complex 3, only one carboxyl group of NTsG takes part in coordination with a bidentate mode.

The size of N-substituent of L-glu has a tremendous impact on MOFs construction. When the R substituent is carbamyl group, a homochiral interpenetrated 3D framework 1 with a pair quadruple helices was obtained. Although fourfold interpenetration has occurred in complex 1, there still exist one-dimensional channels along the *c* axis (Figure 1d). The effective aperture sizes of the two open channels are approximately 0.7 nm × 0.7 nm and 0.4 nm × 0.3 nm, respectively. The accessible void of 1 calculated by PLATON/SOLV¹⁸ analysis is estimated to be 20% without consideration of the H₂O molecules. As the single 3D structure of 1 has large windows viewed down the *a*- and *b*-axes, we consider introducing a more sterically hindered N-substituent of L-glu to effectively prohibit framework interpenetration. If successful, the homochiral MOFs with large pores will have potential applications such as in chiral separation. So the NBzG was used instead of NCG. Interestingly, a non-interpenetrated 3D structure with single-stranded helices has been prepared, however, the topological structure of which is different from complex 1 to a certain degree (cfs via dia). The interpenetration has been effectively suppressed, but unfortunately, the benzoyl group occupied the only remaining 1D channel, which causes 2 to have no free volume. Further increasing the substituent of L-glu with the *p*-tolylsulfonyl group, a novel homochiral bpee-Zn(II) linear chain has been obtained, with NTsG docking at Zn(II). By adjusting the N-substituent of L-glu, pairs of quadruple- to single-stranded helices to lines in the mixed-ligand system have been observed (Scheme 2). More

Scheme 2. From Pair Quadruple- to Single-Stranded Helices to Lines in a Mixed Ligand System via Adjusting the N-Substituent Group of L-Glu



fascinating frameworks and helical chains may be generated by further modifying the R-group or changing the bpee ligand, which is being undertaken by our group. This method should also be promoted to other mixed-ligand systems.

Powder X-ray Diffraction and Thermal Stabilities of the Three Complexes. In order to confirm the phase purity of these complexes, PXRD of complexes 1–3 were measured at room temperature. The experimental PXRD patterns of complexes 1–3 are in good agreement with the simulated ones calculated from the single-crystal diffraction data, indicating that they are in a pure phase (Figures S4–S6, Supporting Information).

To determine the thermal stability of the three complexes, thermogravimetric (TG) measurements were performed in a N₂ atmosphere. TG curves of 1–3 are shown in Figure S7 in the Supporting Information. Complexes 1–3 remained stable up to 210, 291, and 203 °C, respectively. The TGA curve of complex 1 indicates that the loss of H₂O molecules occurs

between 84 and 153 °C (found 5.50%, calc. 5.82%). In complex 2, no weight loss has been found before 291 °C, while a weight loss of 6.55% (calc. 6.18%) was observed in complex 3 with respect to the losses of water molecules.

Circular Dichroism and Nonlinear Optical Properties.

Given that the homochiral complexes 1–3 crystallize in chiral space groups, their solid-state circular dichroism spectra (CD) were studied. As seen in Figure 4a, the CD spectrum of

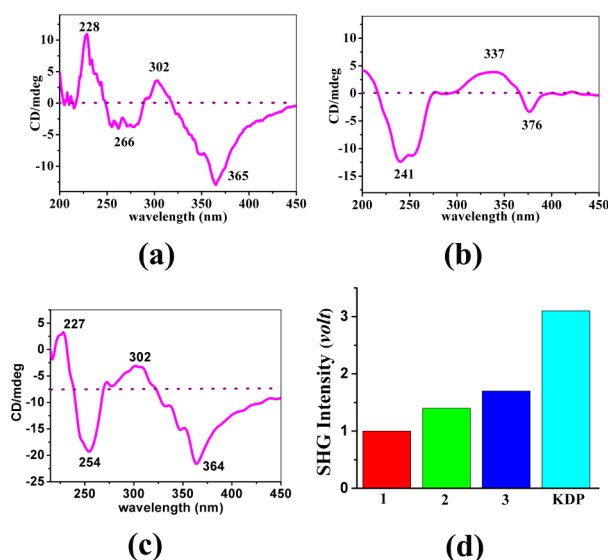


Figure 4. Solid-state CD spectra of samples 1 (a), 2 (b), and 3 (c). (d) Comparison of the measured SHG efficiencies of complexes 1–3 with that of KDP.

complex 1 shows a positive Cotton effect with peaks around 228 and 302 nm, and a negative Cotton effect around 266 and 365 nm; while complex 2 displays a positive CD signal at 337 nm, and negative CD signals at 241 and 376 nm (Figure 4b). Complex 3 exhibits a positive Cotton effect with peaks at 227 and 302 nm, and a negative Cotton effect around 254 and 364 nm (Figure 4c). The results confirm their homochiral nature, which is in good accord with the structures obtained by single-crystal X-ray diffraction.

Second harmonic generation (SHG) active MOFs or CPs, combining the advantages of the organic ligands and metal ions, have attracted great interest due to their potential applications in electric-optical devices, light modulators, and information storage.^{19,5h} Complexes 1–3 are chiral CPs; therefore, their second-order nonlinear optical (NLO) properties were studied by using a Nd:YAG laser (1064 nm). SHG measurements on microcrystalline samples of the three compounds were carried out by using the Kurtz–Perry method²⁰ at room temperature. The results show that complexes 1–3 display SHG efficiencies, which are about 0.32, 0.45, and 0.55 times that of KDP powder in the particle size of 106–150 μm (Figure 4d and Figure S8, Supporting Information), indicating the obvious effects of the chirality on the SHG efficiency in complexes 1–3. The change tendency of NLO properties and structures seems closely related, so we not only can prepare the diverse frameworks but also can adjust their NLO properties by altering the N-substituent of L-glu in this mixed ligand system.

CONCLUSION

In summary, the mixed-ligand strategy, cooperation of an achiral and a chiral ligand, has been shown to be efficient in the preparation of novel homochiral and helical structures. By applying such methodology, homochiral coordination polymers 1–3 have been self-assembled from bpee and three L-glu derivatives under mild conditions. Complex 1 is a 4-fold-interpenetrated 3D framework with paired quadruple-stranded helices; while complex 2 is a non-interpenetrated 3D structure with single-stranded helices. By further increasing the size of N-substituent of L-glu (from carbamyl to benzoyl to *p*-tolylsulfonyl), an interesting linear chain of complex 3 has been obtained. The steric hindrance of the N-substituent of L-glu greatly affects the structures of the CPs and their helical (or linear) chains. More diverse homochiral frameworks and helix may be constructed if adjusting the N-substituent group of L-glu. Other mixed-chiral and achiral ligand systems and the applications of these homochiral CPs are being investigated in our group.

ASSOCIATED CONTENT

Supporting Information

Additional tables, PXRD, TGA, and additional figures. This material is available free of charge via the Internet at <http://pubs.acs.org>.

AUTHOR INFORMATION

Corresponding Author

*E-mail: wxt@fjirsm.ac.cn. Fax: (+) 86-591-83719238.

Notes

The authors declare no competing financial interest.

ACKNOWLEDGMENTS

We are grateful for the financial support of the Major State Basic Research Development Program of China (973 Program, 2012CB821702 and 2014CB845603), the National Science Foundation of China (21173223, 21203194, and 21233009), and Fujian Province (2013J05039).

REFERENCES

- (1) Watson, J. D.; Crick, F. H. C. *Nature* **1953**, *171*, 737–738.
- (2) Nakano, T.; Okamoto, Y. *Chem. Rev.* **2001**, *101*, 4013–4038.
- (3) (a) Ngo, H. L.; Lin, W. *J. Am. Chem. Soc.* **2002**, *124*, 14298–14299. (b) Hu, A.; Ngo, H. L.; Lin, W. *Angew. Chem., Int. Ed.* **2003**, *42*, 6000–6003. (c) Hu, A.; Ngo, H. L.; Lin, W. *J. Am. Chem. Soc.* **2003**, *125*, 11490–11491. (d) Hu, A.; Ngo, H. L.; Lin, W. *Angew. Chem., Int. Ed.* **2004**, *43*, 2501–2504. (e) Wu, C.-D.; Hu, A.; Zhang, L.; Lin, W. *J. Am. Chem. Soc.* **2005**, *127*, 8940–8941. (f) Horike, S.; Dinca, M.; Tamaki, K.; Long, J. R. *J. Am. Chem. Soc.* **2008**, *130*, 5854–5855. (g) Banerjee, M.; Das, S.; Yoon, M.; Choi, H. J.; Hyun, M. H.; Park, S. M.; Seo, G.; Kim, K. *J. Am. Chem. Soc.* **2009**, *131*, 7524–7525. (h) Ma, L.; Abney, C.; Lin, W. *Chem. Soc. Rev.* **2009**, *38*, 1248–1256. (i) Yoon, M.; Shirambalaji, R.; Kim, K. *Chem. Rev.* **2012**, *112*, 1196–1231. (j) Zhu, C. F.; Yuan, G. Z.; Chen, X.; Yang, Z. W.; Cui, Y. *J. Am. Chem. Soc.* **2012**, *134*, 8058–8061. (k) Wu, P.; He, C.; Wang, J.; Peng, X.; Li, X.; An, Y.; Duan, C. *J. Am. Chem. Soc.* **2012**, *134*, 14991–14999. (l) Mo, K.; Yang, Y.; Cui, Y. *J. Am. Chem. Soc.* **2014**, *136*, 1746–1749. (m) Liu, Y.; Xi, X. B.; Ye, C. C.; Gong, T. F.; Yang, Z. W.; Cui, Y. *Angew. Chem., Int. Ed.* **2014**, *53*, 13821–13825.
- (4) (a) Seo, J. S.; Whang, D.; Lee, H.; Jun, S. I.; Oh, J.; Jeon, Y. J.; Kim, K. *Nature* **2000**, *404*, 982–986. (b) Evans, O. R.; Ngo, H. L.; Lin, W. *J. Am. Chem. Soc.* **2001**, *123*, 10395–10396. (c) Xiong, R.-G.; You, X.-Z.; Abrahams, B. F.; Xue, Z.; Che, C.-M. *Angew. Chem., Int. Ed.* **2001**, *40*, 4422–4425. (d) Li, G.; Yu, W.; Cui, Y. *J. Am. Chem. Soc.*

- 2008**, *130*, 4582–4583. (e) Yuan, G.; Zhu, C.; Xuan, W.; Cui, Y. *Chem.—Eur. J.* **2009**, *15*, 6428–6434. (f) Liu, T.; Liu, Y.; Xuan, W.; Cui, Y. *Angew. Chem., Int. Ed.* **2010**, *49*, 4121–4124. (g) Xie, S.-M.; Zhang, Z.-J.; Wang, Z.-Y.; Yuan, L.-M. *J. Am. Chem. Soc.* **2011**, *133*, 11892–11895. (h) Li, J. R.; Sculley, J. L.; Zhou, H. C. *Chem. Rev.* **2012**, *112*, 869–932. (i) Suh, K.; Yutkin, M. P.; Dybtsev, D. N.; Fedin, V. P.; Kim, K. *Chem. Commun.* **2012**, *48*, 513–515. (j) Xuan, W.; Zhang, M.; Liu, Y.; Chen, Z.; Cui, Y. *J. Am. Chem. Soc.* **2012**, *134*, 6904–6907. (k) Wanderley, M. M.; Wang, C.; Wu, C. D.; Lin, W. B. *J. Am. Chem. Soc.* **2012**, *134*, 9050–9053.

- (5) (a) Davis, M. E. *Nature* **2002**, *417*, 813–821. (b) Cui, Y.; Lee, S. J.; Lin, W. B. *J. Am. Chem. Soc.* **2003**, *125*, 6014–6015. (c) Gao, E. Q.; Yue, Y. F.; Bai, S. Q.; He, Z.; Yan, C. H. *J. Am. Chem. Soc.* **2004**, *126*, 1419–1429. (d) Anokhina, E. V.; Go, Y. B.; Lee, Y.; Vogt, T.; Jacobson, A. J. *J. Am. Chem. Soc.* **2006**, *128*, 9957–9962. (e) Dybtsev, D. N.; Nuzhdin, A. L.; Chun, H.; Bryliakov, K. P.; Talsi, E. P.; Fedin, V. P.; Kim, K. *Angew. Chem., Int. Ed.* **2006**, *45*, 916–920. (f) Maspoch, D.; Ruiz-Molina, D.; Veciana, J. *Chem. Soc. Rev.* **2007**, *36*, 770–818. (g) Liu, Y.; Xuan, W. M.; Cui, Y. *Adv. Mater.* **2010**, *22*, 4112–4135. (h) Wang, C.; Zhang, T.; Lin, W. B. *Chem. Rev.* **2012**, *112*, 1084–1104.

- (6) (a) Kepert, C. J.; Prior, T. J.; Rosseinsky, M. J. *J. Am. Chem. Soc.* **2000**, *122*, 5158–5168. (b) Zhang, J.; Bu, X. H. *Angew. Chem., Int. Ed.* **2007**, *46*, 6115–6118. (c) Zhang, J.; Chen, S.; Valle, H.; Wong, M.; Austria, C.; Cruz, M.; Bu, X. *J. Am. Chem. Soc.* **2007**, *129*, 14168–14169. (d) Yuan, G.; Zhu, C.; Liu, Y.; Xuan, W.; Cui, Y. *J. Am. Chem. Soc.* **2009**, *131*, 10452–10460. (e) Ma, L.; Falkowski, J. M.; Abney, C.; Lin, W. B. *Nat. Chem.* **2010**, *2*, 838–846. (f) Song, F. J.; Wang, C.; Falkowski, J. M.; Ma, L. Q.; Lin, W. B. *J. Am. Chem. Soc.* **2010**, *132*, 15390–15398. (g) Xi, X.; Fang, Y.; Dong, T.; Cui, Y. *Angew. Chem., Int. Ed.* **2011**, *50*, 1154–1158. (h) Lun, D. J.; Waterhouse, G. I. N.; Telfer, S. G. *J. Am. Chem. Soc.* **2011**, *133*, 5806–5809. (i) Wen, Y. H.; Sheng, T. L.; Hu, S. M.; Ma, X.; Tan, C. H.; Wang, Y. L.; Sun, Z. H.; Xue, Z. Z.; Wu, X. T. *Chem. Commun.* **2013**, *49*, 10644–10646. (j) Li, P.; He, Y.; Guang, J.; Weng, L.; Zhao, J. C.-G.; Xiang, S.; Chen, B. *J. Am. Chem. Soc.* **2014**, *136*, 547–549.

- (7) (a) Ezuhara, T.; Endo, K.; Aoyama, Y. *J. Am. Chem. Soc.* **1999**, *121*, 3279–3283. (b) Bradshaw, D.; Prior, T. J.; Cussen, E. J.; Claridge, J. B.; Rosseinsky, M. J. *J. Am. Chem. Soc.* **2004**, *126*, 6106–6114. (c) Pérez-García, L.; Amabilino, D. B. *Chem. Soc. Rev.* **2007**, *36*, 941–967. (d) Lin, Z.; Slawin, A. M. Z.; Morris, R. E. *J. Am. Chem. Soc.* **2007**, *129*, 4880–4881. (e) Zhang, J.; Chen, S.; Wu, T.; Feng, P.; Bu, X. *J. Am. Chem. Soc.* **2008**, *130*, 12882–12883. (f) Morris, R. E.; Bu, X. *Nat. Chem.* **2010**, *2*, 353–361. (g) Dang, D. B.; Wu, P. Y.; He, C.; Xie, Z.; Duan, C. Y. *J. Am. Chem. Soc.* **2010**, *132*, 14321–14323. (h) Zhang, J.; Chen, S.; Nieto, R. A.; Wu, T.; Feng, P.; Bu, X. *Angew. Chem., Int. Ed.* **2010**, *49*, 1267–1270. (i) Jing, X.; He, C.; Dong, D.; Yang, L.; Duan, C. *Angew. Chem., Int. Ed.* **2012**, *51*, 10127–10131. (j) Bisht, K. K.; Suresh, E. *J. Am. Chem. Soc.* **2013**, *135*, 15690–15693. (k) Wen, Y. H.; Sheng, T. L.; Sun, Z. H.; Xue, Z. Z.; Wang, Y. L.; Wang, Y.; Hu, S. M.; Ma, X.; Wu, X. T. *Chem. Commun.* **2014**, *50*, 8320–8323.

- (8) Wu, S. T.; Wu, Y. R.; Kang, Q. Q.; Zhang, H.; Long, L. S.; Zheng, Z.; Huang, R. B.; Zheng, L. S. *Angew. Chem., Int. Ed.* **2007**, *46*, 8475–8479.

- (9) (a) Xiao, D. R.; Li, Y. G.; Wang, E. B.; Fan, L. L.; An, H. Y.; Su, Z. M.; Xu, L. *Inorg. Chem.* **2007**, *46*, 4158–4166. (b) Wang, S. N.; Xing, H.; Li, Y. Z.; Bai, J. F.; Scheer, M.; Pan, Y.; You, X. Z. *Chem. Commun.* **2007**, 2293–2295. (c) Hu, Y. W.; Li, G. H.; Liu, X. M.; Hu, Bin.; Bi, M. H.; Gao, L.; Shi, Z.; Feng, S. H. *CrystEngComm* **2008**, *10*, 888–893. (d) Zingiryan, A.; Zhang, J.; Bu, X. H. *Inorg. Chem.* **2008**, *47*, 8607–8609. (e) Qin, C.; Wang, X. L.; Yuan, L.; Wang, E. B. *Cryst. Growth Des.* **2008**, *8*, 2093–2095. (f) Feng, R.; Jiang, F. L.; Chen, L.; Yan, C. F.; Wu, M. Y.; Hong, M. C. *Chem. Commun.* **2009**, 5296–5298. (g) Song, Y. J.; Kwak, H.; Lee, Y. M.; Kim, S. H.; Lee, S. H.; Park, B. K.; Jun, J. Y.; Yu, S. M.; Kim, C.; Kim, S.-J.; Kim, Y. *Polyhedron* **2009**, *28*, 1241–1252. (h) Sun, D.; Li, Y. H.; Hao, H. J.; Liu, F. J.; Wen, Y. M.; Huang, R. B.; Zheng, L. S. *Cryst. Growth Des.* **2011**, *11*, 3323–3327. (i) Chu, Q.; Su, Z.; Fan, J.; Okamura, T.-a.; Lv, G.-C.; Liu, G.-X.; Sun, W.-Y.; Ueyama, N. *Cryst. Growth Des.* **2011**, *11*, 3885–3894.

(j) Cheng, P. C.; Kuo, P. T.; Xie, M. Y.; Hsu, W.; Chen, J. D. *CrystEngComm* **2013**, *15*, 6264–6272. (k) Cao, L.-H.; Wei, Y.-L.; Yang, Y.; Xu, H.; Zang, S. Q.; Hou, H.-W.; Mak, T. C. W. *Cryst. Growth Des.* **2014**, *14*, 1827–1838.

(10) (a) Chen, X. M.; Liu, G. F. *Chem.—Eur. J.* **2002**, *8*, 4811–4817. (b) Martin, D. P.; Staples, R. J.; LaDuca, R. L. *Inorg. Chem.* **2008**, *47*, 9754–9756. (c) Liu, G. X.; Zhu, K.; Xu, H.-M.; Nishihara, S.; Huang, R. Y.; Ren, X. M. *CrystEngComm* **2009**, *11*, 2784–2796. (d) Dong, Z.; Wang, Y. Y.; Liu, R. T.; Liu, J. Q.; Cui, L.; Shi, Q. Z. *Cryst. Growth Des.* **2010**, *10*, 3311–3314. (e) Qin, L.; Zhang, M. D.; Yang, Q. X.; Li, Y. Z.; Zheng, H. G. *Cryst. Growth Des.* **2013**, *13*, 5045–5049. (f) Li, S. B.; Sun, W. L.; Wang, K.; Ma, H. Y.; Pang, H. J.; Liu, H.; Zhang, J. X. *Inorg. Chem.* **2014**, *53*, 4541–4547.

(11) (a) Vaidhyanathan, R.; Bradshaw, D.; Rebilly, J. N.; Barrio, J. P.; Gould, J. A.; Berry, N. G.; Rosseinsky, M. J. *Angew. Chem., Int. Ed.* **2006**, *45*, 6495–6499. (b) Dybtsev, D. N.; Yutkin, M. P.; Peresyphkina, E. V.; Virovets, A. V.; Serre, C.; Férey, G.; Fedin, V. P. *Inorg. Chem.* **2007**, *46*, 6843–6845. (c) Liang, X.-Q.; Li, D.-P.; Zhou, X.-H.; Sui, Y.; Li, Y.-Z.; Zuo, J.-L.; You, X.-Z. *Cryst. Growth Des.* **2009**, *9*, 4872–4883. (d) Zheng, X.-D.; Lu, T.-B. *CrystEngComm* **2010**, *12*, 324–336.

(12) Wen, Y. H.; Sheng, T. L.; Xue, Z. Z.; Sun, Z. H.; Wang, Y. L.; Hu, S. M.; Huang, Y. H.; Li, J.; Wu, X. T. *Cryst. Growth Des.* **2014**, *14*, 6230–6238.

(13) (a) Ingleson, M. J.; Barrio, J. P.; Bacsa, J.; Dickinson, C.; Park, H.; Rosseinsky, M. J. *Chem. Commun.* **2008**, 1287–1289. (b) Barrio, J. P.; Rebilly, J.-N.; Carter, B.; Bradshaw, D.; Bacsa, J.; Ganin, A. Y.; Park, H.; Trewin, A.; Vaidhyanathan, R.; Cooper, A. I.; Warren, J. E.; Rosseinsky, M. J. *Chem.—Eur. J.* **2008**, *14*, 4521–4532. (c) Rood, J. A.; Noll, B. C.; Henderson, K. W. *J. Solid State Chem.* **2010**, *183*, 270–276. (d) Nagaraja, C. M.; Haldar, R.; Maji, T. K.; Rao, C. N. R. *Cryst. Growth Des.* **2012**, *12*, 975–981. (e) Yutkin, M. P.; Zavakhina, M. S.; Samsonenko, D. G.; Dybtsev, D. N.; Fedin, V. P. *Inorg. Chim. Acta* **2013**, *394*, 367–372.

(14) (a) Corradia, A. B.; Lusvardia, G.; Menabuea, L.; Saladinia, M.; Sgarabottob, P. *Polyhedron* **1999**, *18*, 1975–1982. (b) He, R.; Song, H. H.; Wei, Z.; Zhang, J. J.; Gao, Y. Z. *J. Solid State Chem.* **2010**, *183*, 2021–2026. (c) He, R.; Song, H. H.; Wei, Z. *Inorg. Chim. Acta* **2010**, *363*, 2631–2636. (d) Feng, Q.; Yan, M. J.; Song, H. H.; Shi, S. K. *Inorg. Chim. Acta* **2014**, *415*, 75–80.

(15) Sheldrick, G. M. SADABS; University of Göttingen: Göttingen, Germany, 1996.

(16) Sheldrick, G. M. *Acta Crystallogr., Sect. A* **2008**, *64*, 112.

(17) (a) Bassett, A. P.; Magennis, S. W.; Glover, P. B.; Lewis, D. J.; Spencer, N.; Parsons, S.; Williams, R. M.; Cola, L. D.; Pikramenou, Z. *J. Am. Chem. Soc.* **2004**, *126*, 9413–9424. (b) Lin, M. J.; Jouaiti, A.; Kyritsakas, N.; Hosseini, M. W. *Chem. Commun.* **2010**, 46, 115–117. (c) Sahoo, H. S.; Chand, D. K. *Dalton Trans.* **2010**, 39, 7223–7225. (d) Wang, X. F.; Zhang, Y. B.; Lin, Y. Y. *CrystEngComm* **2013**, *15*, 3470–3477. (e) Hou, L.; Jia, L. N.; Shi, W. J.; Du, L. Y.; Li, J.; Wang, Y. Y.; Shi, Q. Z. *Dalton Trans.* **2013**, 42, 6306–6309. (f) Chen, Y. Q.; Li, G. R.; Chang, Z.; Qu, Y. K.; Zhang, Y. H.; Bu, X. H. *Chem. Sci.* **2013**, *4*, 3678–3682.

(18) Spek, A. L. *J. Appl. Crystallogr.* **2003**, *36*, 7–13.

(19) (a) Crassous, J. *Chem. Soc. Rev.* **2009**, *38*, 830–845. (b) Zhang, W.; Xiong, R. G. *Chem. Rev.* **2012**, *112*, 1163–1195.

(20) Kurtz, S. K.; Perry, T. T. *J. Appl. Phys.* **1968**, *39*, 3798–3813.